

OPTICAL PROPERTIES, PHOTOCATALYTIC AND BACTERICIDE ACTIVITY OF PURE AND Ag-DECORATED Zr, Al-DOPED ZnO

¹Leonid AKHKOZOV, ¹Oksana GORBAN, ¹Igor DANILENKO, ¹Sergii GORBAN,
¹Galina VOLKOVA, ¹Iryna BRYUKHANOVA, ²Olesya SHAPOVALOVA, ³Sergii LYUBCHIK,
¹Tetyana KONSTANTINOVA

¹Materials science department, Donetsk institute for physics and engineering NAS of Ukraine, Kyiv, Ukraine,
akhkleo@gmail.com

²REQUIMTE, Associated Laboratory of Green Chemistry, Faculty of Science and Technology, University
Nova de Lisboa, Caparica, Portugal, EU

³NOVA ID FCT, Campus de Caparica, Caparica, Portugal, EU

<https://doi.org/10.37904/nanocon.2019.8535>

Abstract

Structure, optical and photocatalytic properties for wide band gap oxide doped zinc oxide are investigated by XRD, ESR and UV-visible spectroscopy. It was shown the introduction of Al₂O₃ or ZrO₂ led to form of structural defects in zinc oxide matrix. According ESR data a small amount of ZrO₂ (0.01 mol.%) in ZnO forms a defects of donor nature, while the same amount of Al₂O₃ in ZnO matrix led forming as acceptor and as donor defects. Observed tail and shift of optical band gap confirmed ESR data. It was shown the increasing of donor defects in structure ZnO led to increase of photocatalytic activity to phenol degradation. It was shown the dopant types also determined a kind of intermediates of phenol degradation and possible mechanism. For Ag-decorated doped ZnO it is also shown that mechanism of phenol degradation contain a redox cycle. It was shown the bactericide activity of Ag-decorated ZrO₂-doped ZnO to S.aureus is better than E.coli.

Keywords: ZnO, defects, ESR, Ag-decorated ZnO, wide gap oxide doped ZnO, phenol degradation

1. INTRODUCTION

The enhancement of photocatalytic properties for pure oxide is based on decreasing the band gap by the introduction of cationic or/and anionic dopants in the main oxide [1-2]. Usually, this approach is used to enhance the photosensitivity of materials to the visible light [3]. Also, this approach may be used for ions with a variable valence that creates additional centres with oxidative states in catalytic systems [3-4]. There is a wide spectrum of cationic dopants (Ag, Al, Mg, Bi, Cd, Fe, Sn, etc.) uses for the building of catalytic structures based on oxides [5]. However, the comparative analysis of photocatalytic activity for oxides enhanced by different dopants is very difficult because there are many parameters that influence the catalytic activity.

Also, investigators use different kinds of organic pollutants for the estimation of the efficiency of such complex catalysts [6]. A single cationic or anionic dopant [7] may be used, or the cationic and anionic dopants may be combined in zinc oxide [8]. Most investigators use the titanium oxide (TiO₂) system, which is more expensive than the zinc oxide (ZnO) system. Thus, ZnO has a similar or higher catalytic activity and also antibacterial properties [9]. However, ZnO has less stability in water, a high sensitivity to photocorrosion and fast electron-hole recombination [10]. However, ZnO may be modified by wide band gap semiconductors, such as ZrO₂, Al₂O₃ or MgO, which show a high stability to degradation under irradiation. Some studies have noted that Zr-doped ZnO may change the recombination of electron-hole pairs because the Zr atoms provide a deep energy level in the band gap of ZnO [11].

This may give a high hole activity in the modified materials. For Al-doped ZnO, some authors noted that the types of defects in the structure depend on whether the Al atoms substitute for Zn atoms or occupy interstitial

sites [12]. These systems for photovoltaic harvest devices are very well studied. However, the creation of a heterojunction between different oxides of a complex structure may change the structure and surface state of each component. The wide band gap oxides also may enrich the cations of other composite components. As a result, different types of defects in the cationic and anionic sublattice may be created. This may influence the photosensitivity of the wide band gap oxide co-doped ZnO in the near-UV region and the catalytic properties [5,11,13]. Thus, an analysis of recent reviews shows the tendency to use complex composite systems and the less expensive ZnO. Also, there are efforts to solve the problem of ZnO photostability and enhance its catalytic activity [14]. In this work, the influence of Al₂O₃ or ZrO₂ doping on the structure defects, optical and photocatalytic properties will be discussed. In addition, the bactericide activity of Ag-decorated doped ZnO will be addressed.

2. EXPERIMENTAL

Wide gap oxide doped zinc oxide nanoparticles (NPs) were synthesized using a precipitation technique from determined salts in oxalate solution, see **Figure 1**. All used chemicals were of chemical purity. The sediments were washed several times with distilled water before drying in a microwave furnace ($P = 700 \text{ W}$, $f = 2.45 \text{ GHz}$). The dried precipitates were calcined in a resistive furnace at $500 \text{ }^\circ\text{C}$ with a dwell time of 2 h. The amount of doped oxide (ZrO₂ or Al₂O₃) is 0.1 mol. %. The optical properties of ZnO nanopowders were measured on a Cary 5000 UV-Vis-NIR spectrometer with Internal Diffuse Reflectance sphere (Agilent Technologies, USA). Kinetic of 50 ppm phenol solution degradation was estimated by UV spectroscopy and liquid chromatography HPLC. Electron spin resonance (ESR) spectra of systems were obtained on CSM 8400 spectrometers (9.45 GHz). Phase composition was investigated by XRD at CuK _{α} irradiation.

3. RESULTS AND DISCUSSION

The synthesis of the ZnO and (Al₂O₃ or ZrO₂) co-doped ZnO oxide samples involved the sequential forming of the oxide nanoparticles during an isothermal heat-treatment at intervals of $500 \text{ }^\circ\text{C}$. Temperature is a factor for the control of the oxide nanoparticle size, deficiency and surface state [15]. The change of these parameters may be also influence the optical and catalytic properties of the oxides [16,17].

3.1. Wide gap oxide doped ZnO: structure, optical and photocatalytic properties

XRD data was used for estimation of the type and parameters of lattice of pure and doped ZnO. It was shown that all investigated systems crystallized in the wurtzite structure, P63mc. The XRD data shows that the coherent scattering area (CSA) for pure ZnO is 32 nm and the introduction of additional dopant elements does not affect its size in doped zinc oxide.

Table 1 Estimated parameters of cell pure and doped ZnO

Systems	Phase	Cell parameters of ZnO		
		a, Å	c, Å	c/a
ZnO	ZnO, wurtzite	3.2795	5.2025	1.5864
ZnO-0.1 mol. % ZrO ₂	ZnO, wurtzite	3.2603	5.2043	1.5963
ZnO-0.1 mol.% Al ₂ O ₃	ZnO, wurtzite	3.2418	5.2005	1.6042
Ag-ZnO-0.1 mol. % ZrO ₂	Ag, ZnO, wurtzite	3.2608	5.2043	1.5960
Ag-ZnO-0.1 mol.% Al ₂ O ₃	ZnO, wurtzite	3.2482	5.2074	1.6032

At the same time, the parameter a of the ZnO cell decreases with the introduction of dopants, but the parameter c of the ZnO cell shows a slight increase for doped systems in comparison with pure zinc oxide parameters.

This may be due to a decrease in the ionic radii of substituting ions in the ZnO host. The ionic radii of the dopants are $r(\text{Zr}^{4+}) = 0.072 \text{ nm}$, $r(\text{Zr}^{3+}) = 0.084 \text{ nm}$ and $r(\text{Al}^{3+}) = 0.052 \text{ nm}$, while the ionic radius of zinc is 0.076 nm . The change of ratio of c/a for doped systems also correlates with ionic radius of doped element.

Figure 1 shows ESR spectra of doped ZnO systems. For ZrO_2 -doped ZnO the signal with g-factors is equal to 1.9600 is observed in ESR spectrum, as shown in **Figure 1a**.

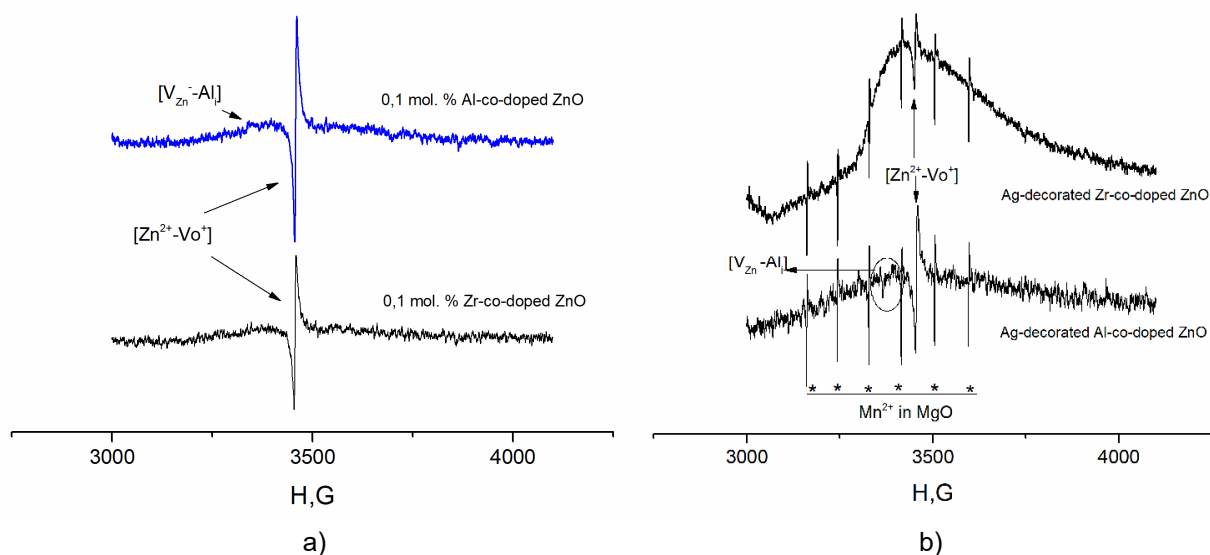


Figure 1 ESR spectra: **a)** for Al_2O_3 and ZrO_2 doped ZnO, **b)** Ag-decorated Al_2O_3 and ZrO_2 doped ZnO

This signal may be superposition of signals from $[\text{Zn}^{2+}-\text{V}_\text{o}^+]$ centers and some amount of $[\text{Zr}^{3+}-\text{V}_\text{o}^{2+}]$ centers in the ZnO structure [18]. The amount of these centers is $2 \cdot 10^{14} \text{ spin/mg}$. Note that for pure ZnO this signal in the ESR spectrum isn't observed. ESR spectrum of 0.1 mol. % Al_2O_3 -doped ZnO shows an isotropic signal with g-factor is equal to 1.9574 ($[\text{Zn}^{2+}-\text{V}_\text{o}^+]$ defects), see **Figure 1a**. The estimated amount of these centers is $4.2 \cdot 10^{14} \text{ spin/mg}$. The signal with $g = 2.0024$ in the ESR spectrum is observed for this system also. This signal may enable the $[\text{V}_{\text{Zn}^-}]$ or $[\text{V}_{\text{Zn}^-} - \text{Zn}_i]$, $[\text{V}_{\text{Zn}^-} - \text{Al}_i]$ centers [19]. Note that the increasing amount of $[\text{Zn}^{2+}-\text{V}_\text{o}^+]$ centers is observed at the transfer from a system with ZrO_2 dopant to system with Al_2O_3 dopant. The defects associated with oxygen vacancies (V_o) should give donor levels in band gap of ZnO, while the defects associated with the second type of defects should give acceptor levels in it.

UV-Vis absorbance spectra for the pure ZnO and Al_2O_3 -doped ZnO, ZrO_2 -doped ZnO are shown in **Figure 2a**. Analysis of UV-Vis absorbance spectra data in coordinate $(h\nu - \text{Abs})^2 - h\nu$ allows estimating of energy of optical band gap of investigated systems. The edge of the adsorption band for pure ZnO is 385 nm ($E_b = 3.19 \text{ eV}$), it is 385 nm ($E_b = 3.19 \text{ eV}$) for ZrO_2 -doped ZnO and it is 390 nm ($E_b = 3.13 \text{ eV}$) for Al_2O_3 -doped ZnO. It is seen the optical band gap of Al_2O_3 -doped ZnO shows the red shift that marks on the presence of acceptor levels in forbidden band of this material. The appearance of tail in the optical spectrum (see inset in **Figure 2a**) indicates on presence of donor levels in band gap of ZnO for all investigated systems. The intensity of tail for Al_2O_3 -doped ZnO is highly compared to other systems. The estimated energy of defect donor levels is near 2.4 eV. It is noted the oxygen vacancies give donor levels in forbidden band of ZnO. These results are confirmed by the ESR data that indicates on the kinds of defects in materials.

Figure 3a shows the photocatalytic activity of pure ZnO, Al_2O_3 -doped ZnO and ZrO_2 -doped ZnO to phenol degradation that estimated based on HPLC data. It is noted that the photocatalytic activity of pure ZnO is close to TiO_2 (P25 Evonik). The estimated rate coefficients (k_{eff} , min^{-1}) on first times degradation (25 min) are

5.19·10⁻² (R²=0.98) for ZnO, 2.9·10⁻² (R²=0.99), for ZrO₂-doped ZnO and 8.32·10⁻² (R²=0.99) for Al₂O₃-doped ZnO.

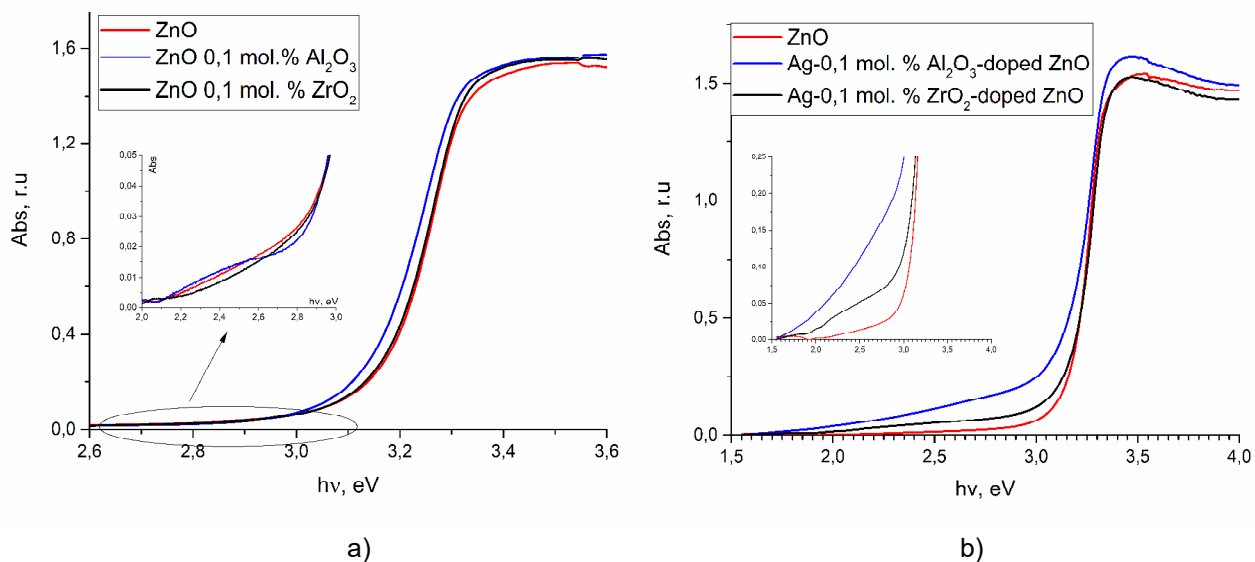


Figure 2 UV-Vis absorbance spectra for a) the pure ZnO and Al₂O₃-doped ZnO, ZrO₂-doped ZnO

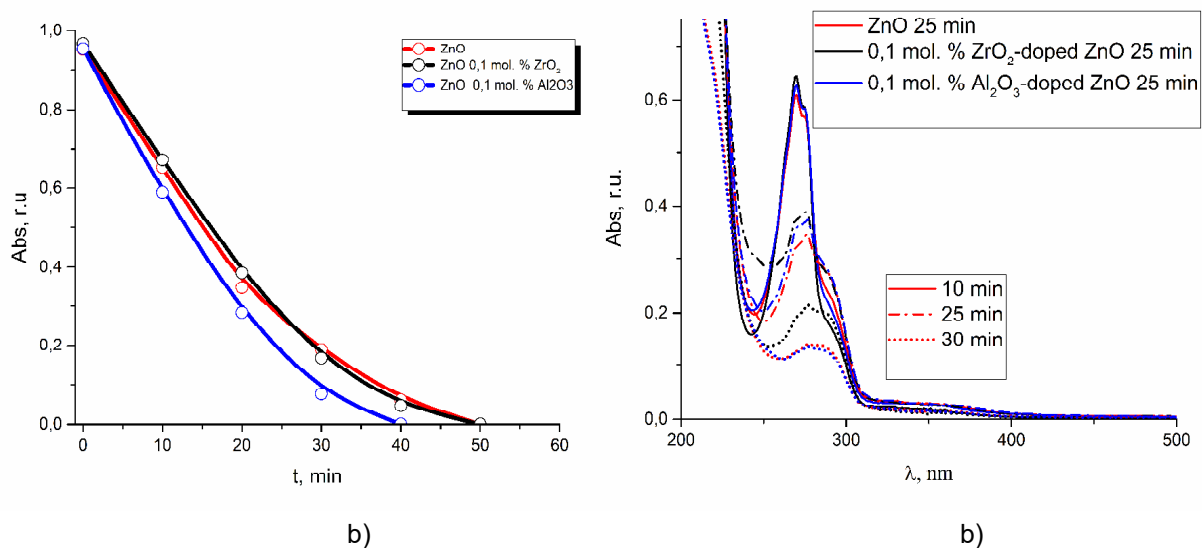


Figure 3 Photocatalytic activity of pure ZnO, Al₂O₃-doped ZnO and ZrO₂-doped ZnO to phenol degradation: a) HPLC data, b) UV-visible spectroscopy and the photocatalytic activity of Ag-decorated ZrO₂-doped ZnO.

It was seen the doping of Al₂O₃ in ZnO enhanced the photocatalytic degradation of phenol in comparison with pure ZnO. It may be connected with the increasing of amount of oxygen vacancies in this material. Phenol degradation in presence of oxides is very well studied [20]. The first mechanism occurs due to hydroquinone formation. Second possible mechanism occurs due to benzoquinone formation with some amounts of hydroquinone, catechol or rezorcin. These compounds have a different wavelength of light adsorption in UV-visible diapason. The analysis of UV-visible spectra of phenol photodegradation by pure and doped ZnO in the time interval of 20-30 min shows the presence of peaks at 270 nm (phenol), 276 nm (1,2-quinone), 254, 289

and 360 nm (1,4-quinone), 244 and 293 nm (hydroquinone). It is noted that the bands corresponding of 1,2-quinone and hydroquinone are more intense in spectra of ZrO₂-doped ZnO and pure ZnO (**Figure 3b**). It was shown the process of phenol photodegradation is close to second mechanism.

3.2. Ag decorated wide gap oxide doped ZnO: structure, optical and photocatalytic properties

According XRD data the AgNPs is forming only in Ag-decorated ZrO₂-doped ZnO. It is noted that Ag doping changes cell parameters only for Al₂O₃-doped ZnO did not change cell parameters (see **Table 1**). The cell parameters of this system are increased. It may be indicate the incorporation in the host lattice of a some amount of silver as Ag⁺ ions with a large ionic radius ($r(\text{Ag}^+) = 0.115 \text{ nm}$). The ESR spectrum of Ag-decorated ZrO₂-doped ZnO shows the appearance of wide signal with $g = 2.03$ which indicates on the formation of surface AgNPs [21]. However, for Ag-decorated Al₂O₃-doped ZnO, ESR signal from surface AgNPs is very weak. It is known that the AgNPs reduce on surface in the presence of Al₂O₃ because the Ag-O-Al strong surface bonds are created in such a host matrix [22].

UV-Vis absorbance spectra for the pure ZnO, Ag-decorated Al₂O₃-doped ZnO and Ag-decorated ZrO₂-doped ZnO are shown in **Figure 2b**. Analysis of UV-Vis absorbance spectra of Ag-decorated systems did not show the changing of the values of optical band gap energies. However, the intensity of tail for Ag-decorated system is higher than for initial undecorated system independently on dopant type and as result the photosensitivity of these materials to visible region irradiation is enhanced. **Figure 4** shows the UV-visible spectra of phenol photodegradation for Ag-decorated systems in which the AgNPs is observed.

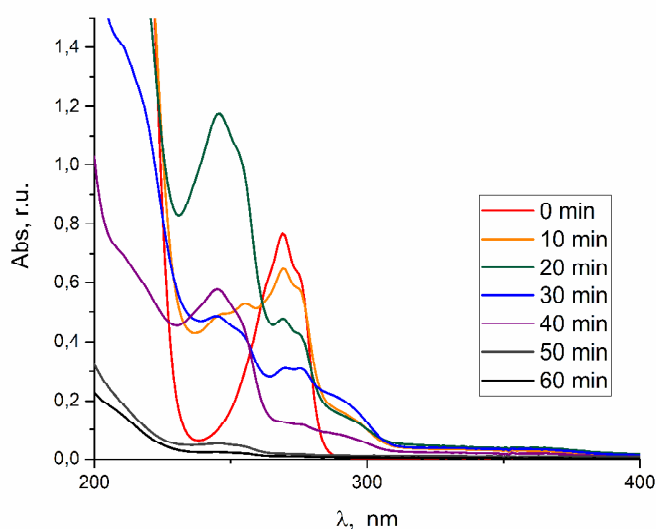


Figure 4 Photocatalytic activity of Ag-decorated ZrO₂-doped ZnO to phenol degradation

As can be seen ZnO based systems and Ag-decorated ZnO based systems show different pattern of phenol degradation. For pure and co-doped ZnO possible mechanism degradation occurs due to benzophenone formation with a small trace hydroquinone, catechol products up to 20 min after start phenol photodegradation. Then the benzophenone destroys due to hydroquinone with simultaneous degradation of last. For Ag-decorated co-doped ZnO systems possible mechanism occur due to hydroquinone formation. The peaks in pattern of phenol degradation at 244 and 293 nm mark the presence of this compound at reaction times up to 20 min. Then the destroying of hydroquinone is observed, see **Figure 4**. It was shown that for Ag-decorated 0.1 mol.% ZrO₂-ZnO the phenol photodegradation occurs due to redox cycle. It is noted the cyclic inversion of 1,4-hydroquinone/1,4-quinone is observed. Two pair Ag⁺/Ag⁰ and 1,4-hydroquinone/1,4-quinone

take part in redox cycle. This slows down the phenol photodegradation. It is also noted that possible mechanism.

The tests for the bactericide activity of Ag-decorated ZrO₂-codoped ZnO show activity to growth inhibition of *S. aureus* (100 %) and *E. coli* (60 %). It was shown that the growth inhibition of *S. aureus* was approximately two times higher than the growth inhibition of *E. coli*.

4. CONCLUSIONS

It was shown, the kind of dopant influences on defects in ZnO structure. Thus, ZrO₂ doping led to form only donor defects in structure, while the Al₂O₃ doping of ZnO forms as acceptor and donor types of defects in ZnO. The defects of structure of doped ZnO are determined the optical properties and photoactivity of ZnO. The formation of surface Ag_m clusters or Ag NPs in doped ZnO depends on the dopant type. It was shown the pure, wide oxide doped ZnO and Ag-decorated doped ZnO have different ways of phenol photodegradation. It was shown that Ag-decorated ZnO has good bactericide properties.

ACKNOWLEDGEMENTS

The authors are thankful for the project N690968 NANOGUARD2AR and project N 47/15H of program NAS of Ukraine "Fundamental problems of creation of new nanomaterials and nanotechnologies" for financial support of their work.

REFERENCES

- [1] KRIVENKO, Pavel.V., KOVALCHUK, G. Yu. Directed synthesis of alkaline aluminosilicate minerals in geocement matrix. *Journal of Materials Science*, 2007, vol. 42, no. 9, p. 2944-29521.
- [2] KUMAR, S. G., DEVI, L. G. Review on Modified TiO₂ Photocatalysis under UV/Visible Light: Selected Results and Related Mechanisms on Interfacial Charge Carrier Transfer Dynamics. *J. Phys. Chem. A*. 2011. 115. P. 13211-13241.
- [3] JOHAR, M. A., AFZAL, R. A., ALAZBA, A. A., MANZOOR, U. Photocatalysis and Bandgap Engineering Using ZnO Nanocomposites. *Advances in Materials Science and Engineering*. 2015. ID 934587: 22.
- [4] 3. ABDO, H. K., NAMRATHA, Q.A., DRMOSH, Z.H., BYRAPP, K. Synthesis of heterostructured Bi₂O₃-CeO₂-ZnO photocatalyst with enhanced sunlight photocatalytic activity. *Ceramics International*. 2017. V. 43. P. 5292-5301.
- [5] HE, R., HOCKING, R. K., TSUZUKI, T. Local structure and photocatalytic property of mechanochemical synthesized ZnO doped with transition metal oxides *J. Austral. Ceram. Soc.* 2013. 49(1). P. 70-75.
- [6] CHONG, M.N, JIN, B., CHOW, C.W.K., SAINT, C. Recent Developments in Photocatalytic Water Treatment Technology A Review. *Water Research*. 2010. 44. p. 2997-3027.
- [7] SHINDE, D. R., TAMBADE, P. S., CHASKAR, M. G., GADAVE, K. M. Photocatalytic degradation of dyes in water by analytical reagent grades ZnO, TiO₂ and SnO₂: a comparative study. *Drink. Water Eng. Sci.* 2017. N10. P. 109-117.
- [8] BOHLE, D. S., SPINA, C. J. Cationic and anionic surface binding sites on nanocrystalline zinc oxide: surface influence on photoluminescence and photocatalysis. *J. Am. Chem. Soc.* 2009. 131. N12. P. 4397-404.
- [9] JENOTTI, A., VAN DE WALL, C.G. Fundamentals of zinc oxide as a semiconductor. *Rep. Prog. Phys.* 2009. 22. P. 26501: 22.
- [10] WANG, L., HU, C., SHAO, L. The antimicrobial activity of nanoparticles: present situation and prospects for the future *Int J Nanomedicin.*, 2017. 12. P. 1227-1229.
- [11] HARIHARAN, C. Photocatalytic degradation of organic contaminants in water by ZnO nanoparticles: Revisited. *Appl. Catal A Chem.* 2006. 304. P. 55-61.

- [12] KHAN, I., KHAN, S., NONGJAI, R., AHMED, H., KHAN, W. Hydrothermal synthesis of zinc oxide powders with controllable morphology. *Optical Materials*. 2013. 35. N6. P. 1189-1193.
- [13] GABAS, M., TORELLI, P., BARRETT, N. T., SACCHI, M., BRUNEVALL, F., CUI, Y., SIMONELLI, L., DÍAZ-CARRASCO, P., RAMOS BARRADO, J. R. Direct observation of Al-doping-induced electronic states in the valence band and band gap of ZnO films. *Phys. Rev. B*. 2011. 84. P. 153303.
- [14] JOSEPH, D. P., VENKATESWARAN, C. Bandgap Engineering in ZnO By Doping with 3D Transition Metal Ions. *Journal of Atomic, Molecular, and Optical Physics*. 2011. 270540:7.
- [15] YANG, Z., ZHANG, P., DING, Y., JIANG, Y., LONG, Z., DAI, W. Facile synthesis of Ag/ZnO heterostructures assisted by UV irradiation: Highly photocatalytic property and enhanced photostability. *Mater. Res. Bull.* 2011. 46. N10. P. 1625-1631.
- [16] KAYANI, Z. N., SALEEMI, F., BATOOL, I. Effect of calcination temperature on the properties of ZnO nanoparticles. *Appl. Phys. A*. 2015. 119. P. 713-720.
- [17] DUTTA, S., CHATTOPADHYAY, S., SARKAR, A., CHAKRABARTI, M., SANYAL, D., JANA, D. Role of Defects in Tailoring Structural, Electrical and Optical Properties of ZnO. *Progress in Materials Science*. 2009. 54.N1. p.89-136.
- [18] JUG, K., TIKHOMIROV, V. A. Influence of intrinsic defects on the properties of zinc oxide. *J Computation Chem*. 2008. 29. N13. P. 2250-2254.
- [19] POLLIOOTTO, V., LIVRAGHI, S., GIAMELLO, E. Electron magnetic resonance as a tool to monitor charge separation and reactivity in photocatalytic materials. *Research on Chemical Intermediates*. 2018. 44. P. 3905-3921.
- [20] ORLINSKII, S. B., SCHMIDT, J., BARANOV, P. G., LORRMANN, V., RIEDEL, I., RAUH, D. AND DYAKONOV V. Identification of shallow Al donors in Al-doped ZnO nanocrystals: EPR and ENDOR spectroscopy. *Phys. Rev. B*. 2008. 77. 115334.
- [21] GRABOWSKA, E., RESZCZYNSKA, J., ZALESKA A. Mechanism of phenol photodegradation in the presence of pure and modified-TiO₂: A review. *Water researcher*. 2012. 46. P. 5453-5471.
- [22] PADLYAK, B.V., KINDRAT, I.I., PADLYAK, T.B., ADAMIV, V.T. Enhancement of the RE³⁺ Luminescence in the RE-Ag Co-doped Tetraborate Glasses. In ELIT-2018. International Scientific and Practical Conference "Electronics and Information Technologies". Lvov: 2018. pp. B37-40.
- [23] SHARMA, N. AND KUMAR, S. Effect of Ag Doping on Properties of Al -Doped ZnO Nanoparticles varies as Zn_{1-x}Ag_xAl_yO. *Mat. Sci. Res. India*. 2017. 14.N2. p. 146-152.